A Model-Based and Data-Driven Integrated Temperature Estimation Method for PMSM

Luhan Jin, *Student Member, IEEE*, Yao Mao, *Member, IEEE*, Xueqing Wang, *Member, IEEE*, Linlin Lu, *Student Member, IEEE*, and Zheng Wang, *Senior Member, IEEE*

***Abstract*—To fulfill accurate online temperature estimation of permanent-magnet synchronous motor (PMSM), an integrated model-based and data-driven method is proposed in this article. First, a simplified lumped parameter thermal network (LPTN) model is developed to learn the tendency of temperature variations. Meanwhile, a small-scale artificial neural network (ANN) is specifically designed to compensate the unmodeled characteristics. The parameters of LPTN model in the proposed method is identified purely from the common variables and no material information is required. With the knowledge learned by the LPTN model and powerful fitting capability of ANN, accurate estimation for both stator and rotor temperatures can be achieved with low computational burden and reduced parameter dependency. Both offline and online experimental results are presented to prove the excellent performances of the proposed method.**

***Index Terms*—Artificial neural network (ANN), lumped parameter thermal network (LPTN), permanent-magnet synchronous motor (PMSM), temperature estimation.**

I. Introduction

THE permanent magnet synchronous motor (PMSM) has been widely applied in various fields owing to its inherent advantages of high efficiency and high-power density [1], [2], [3]. With the increasing demands for high reliability of motor drive, fault diagnosis [4], fault-tolerant control [5], [6], loss optimization [7], [8], [9], and temperature monitoring [10] have been intensively studied. Among them, the research on temperature monitoring is extremely crucial to ensure the safety operation, performance optimization, and parameter estimation [11], [12], [13]. The precise temperature knowledge can be not only used for estimating temperature-dependent machine parameters (e.g., stator resistance), but also combined with the control strategy to maximize the machine power density and self-protection capability.

The machine temperature can be directly measured through infrared thermography and various thermal sensors [14], [15]. However, it is impractical to install the thermal devices in most industrial applications owing to the additional expenses and assembly disadvantages. Against this background, the numerical analysis methods and analytical modeling methods have been intensively investigated in the past decades. The representative numerical analysis methods mainly consist of the finite-element analysis (FEA) and computational fluid dynamics [16], which exhibit high temperature estimation accuracy due to their powerful modeling capability. However, apart from the challenges associated with identifying proper software configuration, the massive computational burden also prohibits them from online implementation. The analytical modeling methods are mainly fulfilled based on the lumped-parameter thermal network (LPTN) [17]. As a noninvasive estimation technique, the LPTN simplifies the intricate thermal behavior and abstracts the heat transfer mechanisms inside the machine system through equivalent circuit principle [18]. Different LPTNs have been established in the existing literatures with lower computational burden [19], [20], [21]. Nevertheless, the performance of these methods usually relies on the geometrical and material parameters of the machine, which can be hardly accessible in practical applications [17]. Under these circumstances, some research groups began to develop the intelligent optimization-assisted low-order LPTNs [18], [22], [23], [24], [25]. In these literatures, different optimization algorithms, including the genetic algorithm and particle swarm optimization (PSO), are employed to search for the optimal LPTN parameters, which can avoid the troublesome parameter determination process. Although the issue of serious parameter dependency can be alleviated to some extent, extra measuring devices are still necessary in these methods to record the power loss information, which increases the system cost. To avoid the use of thermal parameters and detailed loss values, Sheng et al. [26] developed an online prediction model only from the measured data by using the least square method. However, additional distributed sensors and time-consuming data-collection process are required in [26] to guarantee the estimation accuracy, which limits its practicability.

On the other hand, with the advancement of artificial intelligence, the data-driven methods have emerged in the field

Manuscript received 23 November 2023; revised 6 February 2024; accepted 22 March 2024. Date of publication 28 March 2024; date of current version 16 May 2024. This work was supported in part by the National Natural Science Foundation of China under Grant 62303333 and in part by the Science and Technology Projects of Chengdu City under Grant 2022-YF05-00228-SN. Recommended for publication by Associate Editor F. Freijedo. *(Corresponding author: Xueqing Wang.)*

Luhan Jin, Yao Mao, and Linlin Lu are with the National Key Laboratory of Optical Field Manipulation Science and Technology, Chinese Academy of Sciences, Chengdu 610209, China, also with the Key Laboratory of Optical Engineering, Chinese Academy of Sciences, Chengdu 610209, China, also with the Institute of Optics and Electronics, Chinese Academy of Sciences, Chengdu 610209, China, and also with the University of Chinese Academy of Sciences, Beijing 101408, China (e-mail: maoyao@ioe.ac.cn; lulinlin21@mails.ucas.ac.cn).

Xueqing Wang is with the College of Electrical Engineering, Sichuan University, Chengdu 610065, China (e-mail: xwang@scu.edu.cn).

Zheng Wang is with the School of Electrical Engineering, Southeast University, Nanjing 210096, China (e-mail: zwang@eee.hku.hk).

Color versions of one or more figures in this article are available at https://doi.org/10.1109/TPEL.2024.3382300.

Digital Object Identifier 10.1109/TPEL.2024.3382300

of motor temperature estimation [27], [28], [29]. Different from the model-based methods, the data-driven methods can achieve high estimation accuracy without the knowledge of machine information, owing to their powerful fitting capability. Thus, the data-driven methods can still output satisfactory predicted results under the operating states where the physical model assumptions are inaccurate [28]. The data-driven methods also feature several demerits, namely the time-consuming training process of large-scale neural network and considerable online computational resources, which are impractical in most industrial applications.

To resolve the abovementioned problems, an integrated model-based and data-driven method is proposed in this article for precise online temperature estimation of PMSM with low parameter dependency. Specifically, a simplified LPTN model regarding the stator winding and permanent magnet is developed to capture the thermal dynamics of PMSM and provide prior knowledge of the estimated temperatures for the data-driven compensator. After extracting temperature-related features, an artificial neural network (ANN) is designed to compensate the unmodeled characteristics and parameter variations. The parameters of the developed LPTN model are optimized purely from the measurement data and no extra experiments are required to obtain the detailed loss information. By combining the merits of both model-based and data-driven methods, the proposed strategy can fulfill accurate temperature estimation without requiring specific machine information and considerable computing resources, which makes it a practical and superior solution for online motor temperature estimation.

The rest of this article is organized as follows. The preliminary about LPTN is introduced in Section II. Section III briefly presents the general overview of the proposed integrated model-based and data-driven method, and discusses the related details in each subsection. Then, the experimental results are presented and discussed in Section IV. Finally, Section V concludes this article.

II. Preliminaries of LPTN

Similar to the electrical circuit, the LPTN models the heat transfer process of the machine from the thermal perspective, where the elements with identical temperatures are merged to form a single node. The analogy between the electric circuit model and LPTN model is depicted in the Fig. 1. Instead of using electric resistor and capacitor, the thermal resistor and capacitor are employed in the LPTN to reflect the thermal properties and heat storage of different machine components [30], respectively. Furthermore, the current sources and node voltages in the electrical circuit are transformed into power losses and node temperatures in the LPTN model, correspondingly. In this way, well established electric circuit theorems can be directly used in the LPTN model to describe the related thermal behaviors, such as the Kirchhoff's voltage and current laws.

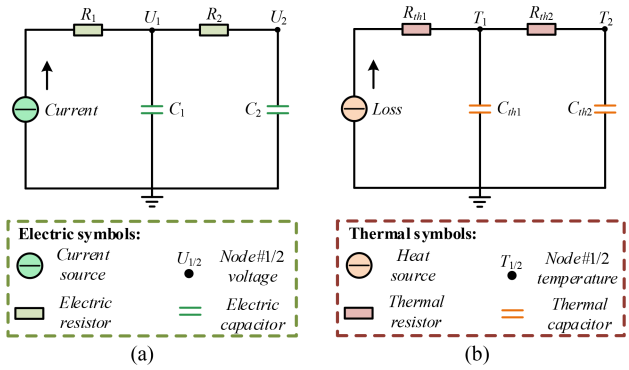

Fig. 1. Comparison between the electric circuit and LPTN. (a) Electric circuit representation. (b) LPTN representation.

III. Proposed Integrated Model-Based and Data-Driven Online Temperature Estimation Method

A. Overview of the Proposed Method

The model-based low-order LPTN methods can learn the tendency of temperature variations with the inherent demerits of serious parameter dependency and lower estimation accuracy, which prevents them from practical applications. Although the number of nodes in the LPTN model can be further increased to improve the estimation performance, the computational burden and parameterization difficulty are also raised. On the other hand, the data-driven approaches can fulfill great estimation precision using only measurement data. However, their generalization performance is limited and heavy computational burden are usually required. To leverage the respective strengths of model-based and data-driven methods, a practical temperature estimation method combining both the model-based and data-driven approaches is proposed in this article to simultaneously eliminate the parameter dependency of the LPTN model and achieve precise temperature estimation with acceptable computational burden.

The overall structure of the proposed framework is presented in Fig. 2. First, the related temperatures including stator temperature T_s, rotor temperature T_r, ambient temperature T_a, coolant temperature T_c, d-q axis currents i_d and i_q, and rotor speed ω_r are measured to establish the LPTN model. No expensive equipment is required to obtain detailed motor loss information. After finishing data collection, the parameterized loss model and LPTN model involving the stator and rotor temperatures are developed and optimized with only measurement data, which avoids extensive testing procedures and prolongs the machine lifetime. Finally, the temperature residuals between the estimated temperatures from the LPTN model and the corresponding real temperatures are calculated accordingly and used for the training of the ANN compensator. In this way, the missing knowledge regarding the model uncertainty can be effectively extracted and applied to the compensation module to improve the estimation accuracy. Detailed descriptions of the model-based part and data-driven part in the proposed method can be found in the following sections.

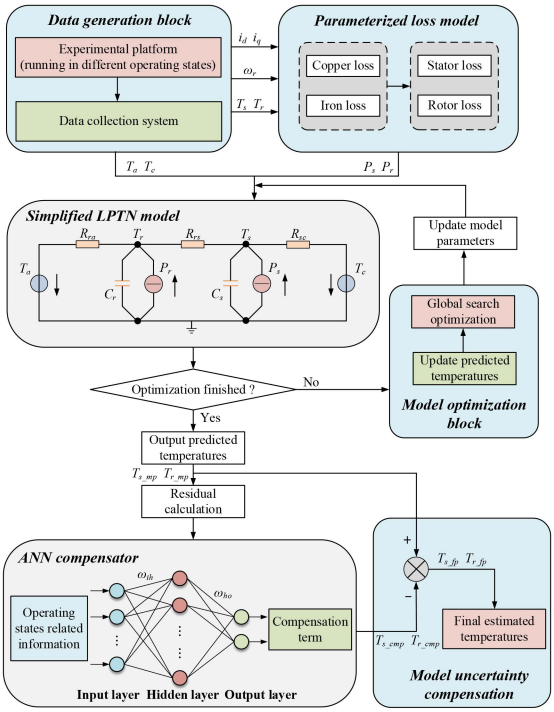

Fig. 2. Overview of the proposed method.

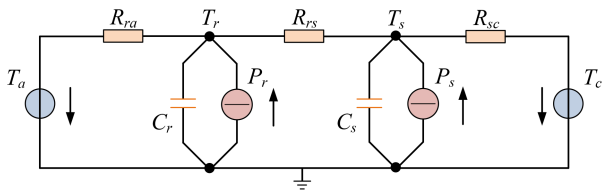

Fig. 3. Representation of the developed LPTN model.

B. Model-Based Part: Simplified LPTN Model

Due to the rich knowledge contained in the thermal model and the fast estimation speed, the use of model-based strategy is indispensable in estimating the machine temperatures. In this article, a simplified two-node LPTN model involving the stator winding temperature T_s and rotor temperature T_r is developed to learn the tendency of temperature variations and extract prior knowledge of estimated temperatures for the ANN compensator, as shown in Fig. 3. T_a and T_c are two measured quantities representing the ambient and coolant temperatures, respectively. The thermal resistance R_{ij} represents the thermal properties between the node i and node j. Meanwhile, each node is linked to the corresponding thermal capacity C_i, which defines the heat storage capability of the node i. The heat sources P_s and P_r refer to the generated thermal losses within the stator and rotor.

Because of the complex machine properties and variable operating states, the calculation of accurate loss values remains a challenging task. The existing LPTN-based methods require extensive experiments or time-consuming FEA simulations to develop a precise loss model for better performance, which limits them from practical applications. By comparison, the parameters of the loss model in this article are optimized purely from the easily measurable data. Since the ANN compensator can learn the mismatch between LPTN model output and real temperatures, the proper simplifications in the loss model and LPTN model will not deteriorate the estimation performance of the proposed method. For the establishment of parameterized loss model, the copper loss P_{Cu} and iron loss P_{Fe} are calculated based on the following equations [31], [32]:

$$\begin{cases} P_{Cu} = 1.5R_s(i_d^2 + i_q^2) \\ P_{Fe} = k_h\omega_r\psi_s^2 + k_e\omega_r^2\psi_s^2 \end{cases} \tag{1}$$

where k_h and k_e are the hysteresis loss and eddy current loss coefficients, respectively. R_s is the temperature-dependent stator resistance that can be expressed as

$$R_s = R_{s,20}[1 + \alpha_{cu,20}(T_s - 20)] \tag{2}$$

where $R_{s,20}$ is the measured stator resistance at 20 °C and $\alpha_{cu,20}$ is the copper temperature coefficient adopted as 0.00393/°C. ψ_s in (1) refers to the stator flux linkage that can be expressed as

$$\psi_s = \sqrt{(L_q i_q)^2 + (L_d i_d + \psi_{PM})^2} \tag{3}$$

where L_d and L_q represent the d-axis and q-axis inductance, respectively. ψ_{PM} is the permanent magnet flux linkage.

After extracting the copper loss and iron loss based on (1), the stator loss P_s and rotor loss P_r can be calculated as

$$\begin{cases} P_s = P_{Cu} + k_{si}P_{Fe} \\ P_r = (1 - k_{si})P_{Fe} \end{cases} \tag{4}$$

where k_{si} indicates the proportion of stator iron loss in the overall iron loss.

By applying the Kirchhoff's voltage and current laws, the state-space representation of the developed LPTN model in Fig. 3 can be derived as

$$\dot{\boldsymbol{T}} = \boldsymbol{A}\boldsymbol{T} + \boldsymbol{B}\boldsymbol{u} \tag{5}$$

with

$$\begin{aligned} \boldsymbol{T} &= [T_s \quad T_r]^t \\ \boldsymbol{u} &= [P_s \quad P_r \quad T_a \quad T_c]^t \\ \boldsymbol{A} &= \boldsymbol{C}^{-1}\begin{bmatrix} -(\frac{1}{R_{rs}} + \frac{1}{R_{sc}}) & \frac{1}{R_{rs}} \\ \frac{1}{R_{rs}} & -(\frac{1}{R_{rs}} + \frac{1}{R_{ra}}) \end{bmatrix} \\ \boldsymbol{B} &= \boldsymbol{C}^{-1}\begin{bmatrix} 1 & 0 & 0 & \frac{1}{R_{sc}} \\ 0 & 1 & \frac{1}{R_{ra}} & 0 \end{bmatrix} \\ \boldsymbol{C} &= \begin{bmatrix} C_s & 0 \\ 0 & C_r \end{bmatrix}. \end{aligned} \tag{6}$$

For online implementation, the state space (5) needs to be discretized. By using the explicit Euler method, the discretized predicting equation can be expressed as

$$\boldsymbol{T}(k+1) = (T_{st}\boldsymbol{A} + \boldsymbol{I}_2)\boldsymbol{T}(k) + T_{st}\boldsymbol{B}\boldsymbol{u} \tag{7}$$

where T_{st} represents the sampling time and $\boldsymbol{I}_2$ is a 2×2 identity matrix.

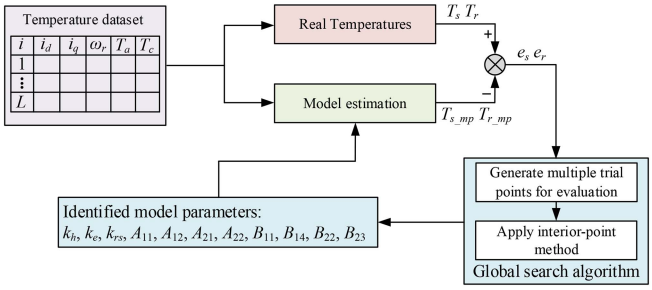

Fig. 4. Parameter identification process.

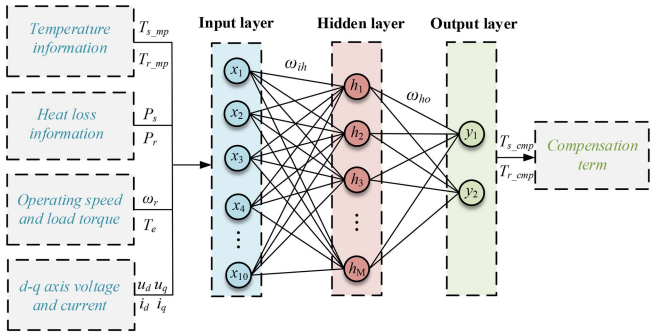

Fig. 5. Architecture of ANN compensator.

For the convenience of optimization, the predicting (7) is further parametrized as

$$\boldsymbol{T}(k+1) = T_{st}\begin{bmatrix} A_{11} & A_{12} \\ A_{21} & A_{22} \end{bmatrix}\boldsymbol{T}(k) + \boldsymbol{T}(k) + T_{st}\begin{bmatrix} B_{11} & 0 & 0 & B_{14} \\ 0 & B_{22} & B_{23} & 0 \end{bmatrix}\boldsymbol{u} \tag{8}$$

where the A_{11}, A_{12}, A_{21}, A_{22}, B_{11}, B_{14}, B_{22}, and B_{23} are the corresponding element in the system matrix $\boldsymbol{A}$ and input matrix $\boldsymbol{B}$, respectively.

There are 11 parameters in the simplified LPTN model required to be identified. In this article, the global search algorithm is employed to find the optimal parameters [33]. The algorithm can achieve excellent optimization performance rapidly by combining both heuristic search and gradient-based methods. Specifically, the global search algorithm generates multiple trial points using the scatter search scheme and evaluates them to choose the potential points for future optimization. Then, the interior-point method will be applied for the second-stage optimization. In order to minimize the temperature estimation error, the optimization problem in this article can be defined as

$$\begin{aligned} \min J(\hat{\boldsymbol{x}}) = \frac{1}{L}\sum_{i=1}^{L}(&||T_s(i) - \hat{T}_s(i,\hat{\boldsymbol{x}})||^2 \\ &+ ||T_r(i) - \hat{T}_r(i,\hat{\boldsymbol{x}})||^2) \\ \text{s.t. } &\boldsymbol{x}_{\min} \le \hat{\boldsymbol{x}} \le \boldsymbol{x}_{\max} \end{aligned} \tag{9}$$

where $\hat{T}_s$ and $\hat{T}_r$ are the predicted stator and rotor temperatures, respectively. L is the number of sampling points. $\boldsymbol{x}_{\min}$ and $\boldsymbol{x}_{\max}$ are the lower and upper bounds of parameter vector $\hat{x}$.

By introducing the barrier function, the original optimization problem (9) with equality constraint can be transformed into an unconstrained optimization problem, as expressed in

$$\min J_b(\hat{\boldsymbol{x}}) = J(\hat{\boldsymbol{x}}) - \mu\ln(\boldsymbol{x}_{\max} - \hat{\boldsymbol{x}}) - \mu\ln(\hat{\boldsymbol{x}} - \boldsymbol{x}_{\min}) \tag{10}$$

where μ refers to the barrier parameter.

With Karush–Kuhn–Tucker conditions, the optimization problem in (10) can be effectively solved using Newton's method [34]. The general parameter identification process of the simplified LPTN model is shown in Fig. 4. It should be mentioned that the utilization of the simplified LPTN model is to capture the tendency of temperature variation and provide prior temperature estimation for the data-driven part. Although the simplified LPTN model will introduce inevitable estimation errors, the subsequent designed ANN compensator can be employed to compensate the model uncertainty to guarantee the estimation precision. Thus, the inaccurate parameters in the simplified LPTN model are acceptable.

C. Data-Driven Part: ANN Compensator

Since the simplified LPTN model will cause inevitable estimation errors, the data-driven strategy is utilized in this article to compensate the model uncertainty. According to the universal approximation theorem [35], a single hidden-layer feedforward ANN can approximate any complex functions with satisfactory precision. Thus, it is employed in the proposed method to extract model uncertainty knowledge. The topology of the ANN compensator is shown in Fig. 5.

As shown in Fig. 5, the input layer of ANN compensator consists of the temperature related information T_{s_mp} and T_{r_mp}, loss related information P_s and P_r, motor speed ω_r and load torque T_e, and d-q axis voltages and currents. Compared with the existing data-driven estimation methods, which utilizes exponentially weighted moving average technique to obtain information by increasing input dimensions, the proposed method can extract effective mapping relationship with fewer data dimensions by utilizing the prior temperature knowledge from the LPTN model. For the output layer, two compensation terms regarding stator and rotor temperatures T_{s_cmp}, T_{r_cmp} are calculated as follows:

$$y_o = \sum_{h=1}^{M}\left\{\omega_{ho}Tsf\left(\sum_{i=1}^{10}\omega_{ih}x_i + b_h\right)\right\} + b_o, \quad o = 1, 2 \tag{11}$$

where ω_{ih} is the weight between the ith input neuron and hth hidden node, ω_{ho} refers to the weight between the hth hidden node and oth output neuron, b_h and b_o represent the bias of hth hidden node and oth output neuron, respectively. M is the number of hidden nodes.

The tangent sigmoid function $Tsf(x)$ in (11) is employed as the activation function in the hidden layer, which can be expressed as

$$Tsf(x) = \frac{2}{1 + e^{-2x}} - 1. \tag{12}$$

It can be concluded from (11) that the mathematical equation of the ANN compensator can be obtained explicitly, which is convenient for online implementation. The training input features in the ANN compensator can be directly obtained from the simplified LPTN model and the corresponding output can be collected by calculating the temperature residuals between the LPTN model output and real temperatures. Thus, the developed ANN compensator can be easily implemented without extra measurements. The training objective of the ANN compensator is to find the optimal weight ω^* and bias $\boldsymbol{b}^*$ that minimize the estimation error of compensation terms. Owing to the fast speed and guaranteed convergence, the Levenberg–Marquardt algorithm is applied to optimize parameters of the ANN compensator [36].

The predicted compensation terms T_{s_cmp} and T_{r_cmp} will be imported to the model uncertainty compensation module in Fig. 2 for final calculation. Specifically, the final predicted stator and rotor temperatures T_{s_fp} and T_{r_fp} can be calculated by subtracting the compensation terms from the temperatures predicted by the simplified LPTN model, as expressed in

$$\begin{bmatrix} T_{s\_fp} \\ T_{r\_fp} \end{bmatrix} = \begin{bmatrix} T_{s\_mp} \\ T_{r\_mp} \end{bmatrix} - \begin{bmatrix} T_{s\_cmp} \\ T_{r\_cmp} \end{bmatrix}. \tag{13}$$

To avoid abrupt oscillations and improve the estimation performance under dynamic operations, a temperature-gradient based smoothing technique is introduced. Theoretically, the real temperature at adjacent sampling time changes slowly. Considering the temperature gradient constraint, the smoothing technique in the proposed method can be expressed as

$$\boldsymbol{T}^k_{fp-smo} = \begin{cases} \boldsymbol{T}^k_{fp}, \text{abs}(\boldsymbol{T}^k_{fp} - \boldsymbol{T}^{k-1}_{fp-smo}) < \Delta \boldsymbol{T}_{\max} \\ \boldsymbol{T}^{k-1}_{fp-smo}, \text{otherwise} \end{cases} \tag{14}$$

where T^k_{fp-smo} is the smoothed predicted temperature vector in kth sampling period, T^k_{fp} is the predicted temperature vector after compensation in the kth sampling period, and $\Delta \boldsymbol{T}_{\max}$ refers to the temperature variation threshold vector.

IV. Experimental Validation

In the experiment, the dataset with a constant sampling rate of 2 Hz collected by the LEA department at Paderborn University is utilized to verify the effectiveness of the proposed method [27]. During the data collection process, since the real temperature cannot change abruptly, it will take some time for the measured temperature to reach its stable value. To acquire precise temperature data, the desired data will be collected only when the measured temperature is stable, which can be ensured by maintaining the current operating state for a certain period. The parameters of the PMSM used in the experiment are listed in Table I.

A. Evaluation of Estimation Accuracy

During the experiment, the parameters of the simplified LPTN model are identified using global search algorithm programmed by MATLAB. To obtain the reasonable parameter values and accelerate the optimization process, the search domains of all model parameters are given in advance. Given that the magnitude of thermal capacity is usually much larger than that of thermal resistance, the maximum search range of the elements in (8) are all limited to $[-1\ 1]$. According to the symbol of different elements, the corresponding search range can be further determined as $[-1\ 0]$ or $[0\ 1]$. Besides, all model parameters are initialized with zero and the number of trial points are set to 500 in this article. The identification results are displayed in Table II.

After finishing parameter identification, 90 000 training samples and 30 000 validation samples are generated to train the ANN compensator. Considering the tradeoff between accuracy and computational efficiency, the number of hidden nodes is selected as 50. For the evaluation of estimation accuracy, 30 000 data samples with multiworking conditions are employed as the testing dataset, which is independent of both training and validation datasets. The multiworking conditions in Fig. 6 include both speed and load torque variations to reflect the estimation performance under rapid dynamic operations. The corresponding results are shown in Fig. 7. During the verification, the temperature

TABLE I
Parameters of The PMSM

Name	Value
Pole pair number	8
d-axis inductance	0.15 mH
q-axis inductance	0.25 mH
PM flux	0.055 Wb
Stator resistance	13 mΩ
Power rating (nom./max.)	22/52 kW
Current rating (nom./max.)	110/283 A
Torque rating (nom./max.)	110/250 Nm
Cooling type	Water-glycol

TABLE II
Parameters Identification Results

Name	Search domain	Identified Value
k_h	[0 1]	8.3×10^{-5}
k_e	[0 1]	0.0151
k_{rs}	[0 1]	0.9871
A_{11}	[-1 0]	-0.0051
A_{12}	[0 1]	3.6×10^{-9}
A_{21}	[0 1]	8.3×10^{-4}
A_{22}	[-1 0]	-0.002
B_{11}	[0 1]	2.4×10^{-4}
B_{14}	[0 1]	0.0052
B_{22}	[0 1]	0.0052
B_{23}	[0 1]	0.0016

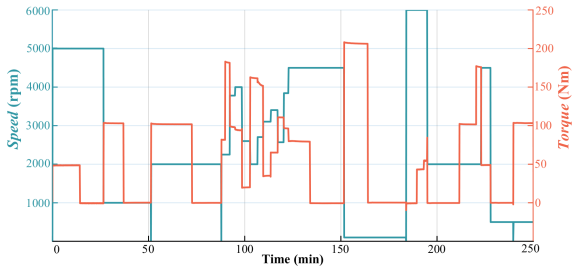

Fig. 6. Multiworking conditions for testing with varying speed and load torque.

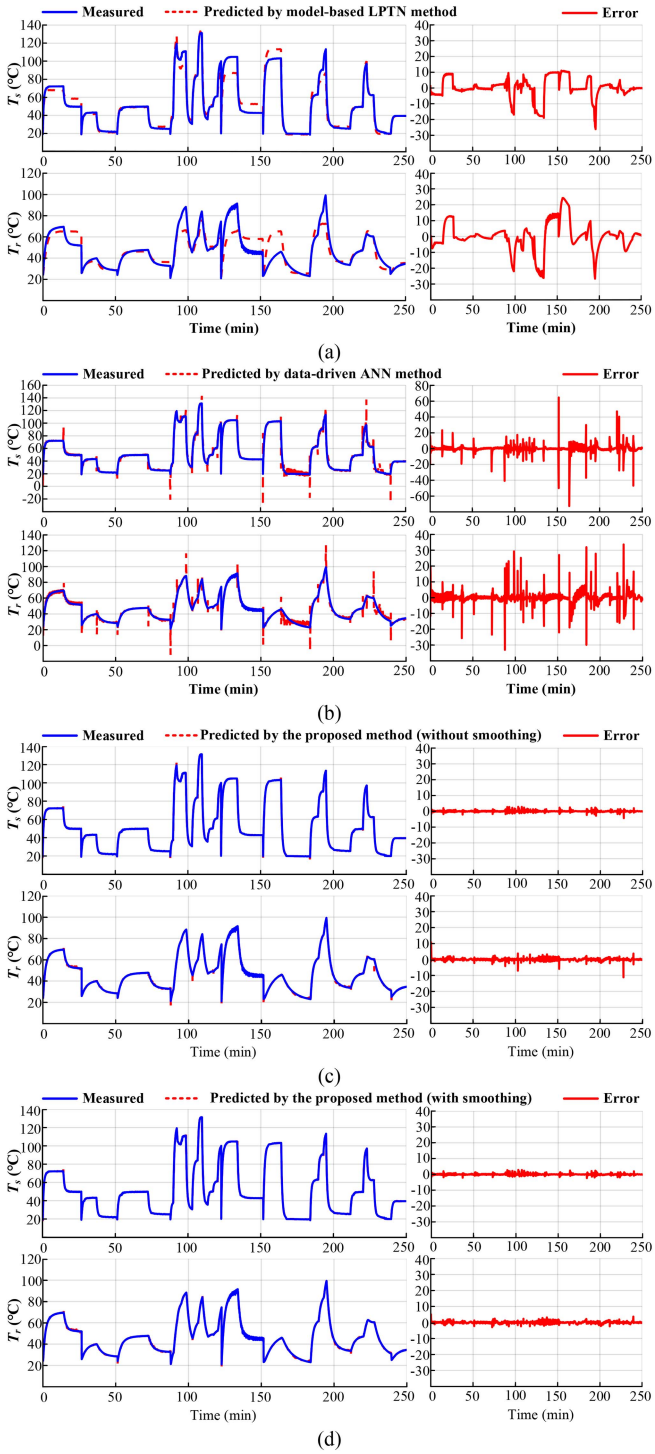

Fig. 7. Estimation performances of different methods. (a) Model-based LPTN method. (b) Data-driven ANN method. (c) Proposed integrated method without smoothing. (d) Proposed integrated method with smoothing.

estimation results using only LPTN model and ANN with same number of hidden nodes are also presented for comparisons to further prove the effectiveness of the proposed method, respectively. As shown in Fig. 7(a), the model-based LPTN method is able to learn the tendency of temperature variation with smooth estimation. However, the estimation error for both stator winding

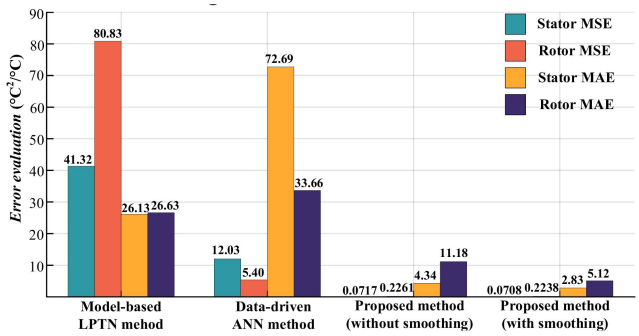

Fig. 8. Comparisons of estimation error statistics.

and rotor are still unacceptable in practical applications owing to the inaccuracy of the modeling process. On the other hand, the data-driven ANN method can well estimate the stator and rotor temperatures with intermittent abrupt oscillations, as shown in Fig. 7(b). Under the rapid dynamic operations shown in Fig. 6, the performance of the ANN method will deteriorate quickly with small number of hidden nodes. For the proposed integrated model-based and data-driven method without smoothing, the estimated temperatures demonstrate excellent agreement with the measured temperatures, as shown in Fig. 7(c). Only slight oscillations occur in the estimated rotor temperatures. After introducing the proposed gradient-based smoothing technique, these oscillations can be further alleviated, as shown in Fig. 7(d). In Fig. 7, with the same training and testing data, the proposed integrated model-based and data-driven method exhibits superior estimation accuracy under both normal and dynamic operations compared with the model-based LPTN method and data-driven ANN method, which proves the effectiveness and superiority of the proposed method. The remarkable estimation performance of the proposed method is attributed to its exceptional ability to exploit the respective strengths of both model-based LPTN method and data-driven method. By integrating the merits of model-based and data-driven methods, the proposed method successfully alleviates the high parameter dependency in the model-based method with improved estimation accuracy and address the unstable estimation problem in the data-driven ANN method with better generalization performance.

In order to prove the superiority of the proposed method quantitatively, the estimation error statistics of different methods are compared in the Fig. 8. During the comparison, two typical evaluation metrics are adopted, i.e., mean squared error (MSE) and maximum absolute error (MAE), which can be expressed as

$$\mathrm{MSE} = \frac{1}{N}\sum_{i=1}^{N} e_i^2$$

$$\mathrm{MAE} = \max\{abs(e_1), abs(e_2), \ldots, abs(e_N)\} \tag{15}$$

where N is the number of testing data and e_i is the estimation error on the ith testing data.

In Fig. 8, the model-based LPTN method has the highest stator and rotor MSEs of 41.32 °C^2 and 80.83 °C^2, with stator and rotor MAEs of 26.13 °C and 26.63 °C, respectively. With

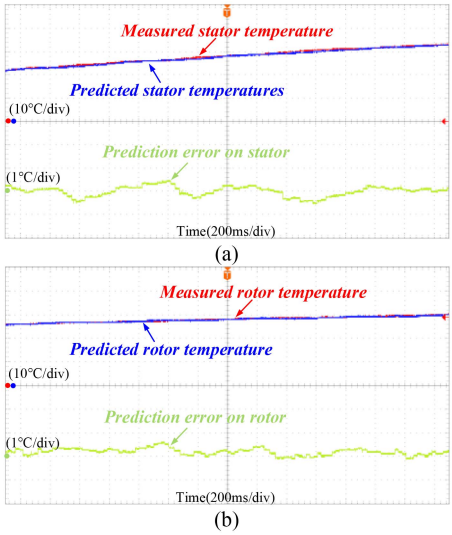

Fig. 9. Online temperature estimation results. (a) Stator. (b) Rotor.

the powerful fitting capability of data-driven ANN method, the stator and rotor MSEs can be reduced to 12.03 °C^2 and 5.40 °C^2, respectively. However, the stator and rotor MAEs are increased to 72.69 °C and 33.66 °C due to the low generalization performance caused by the limited network size. By utilizing the prior temperature knowledge extracted by the LPTN model and powerful fitting capability of ANN, the proposed integrated model-based and data-driven method with smoothing achieves the lowest stator and rotor MSEs of 0.0708 °C^2 and 0.2238 °C^2, with significantly reduced stator and rotor MAEs of 2.83 °C and 5.12 °C, respectively. In conclusion, the experimental results in Figs. 7 and 8 prove that the proposed method can well estimate the stator and rotor temperatures with lower errors.

B. Online Verification

To prove the feasibility of the proposed method for real-time estimation, the online estimation experiments are performed in the common industrial microcontroller DSP (TMS320F28335) with the main frequency of 150 MHz. In the real-time experiments, the acquisition of online sampled data is simulated by importing the previously collected data into the DSP and feeding it into the proposed method during each sampling period, which is equivalent to using the real-time sampled data. The real-time temperature estimation results of the proposed method are shown in Fig. 9. The proposed method only consumes approximately 0.4 ms to fulfill each estimation. Additionally, the estimated stator and rotor temperatures match their respective measured values excellently and the maximum estimation errors are within 1 °C, as shown in Fig. 9. The successful implementation of real-time experiments in DSP and fast estimation time can jointly verify that the proposed method can be easily applied for real-time estimation in common industrial microcontrollers with low computational burden.

C. Performance Comparison

The proposed method is also compared with the existing state-of-the-art model-based methods [24], [26] and data-driven methods [28], [29] in terms of estimation accuracy, calculation speed, parameter dependency, and implementation complexity, as shown in Table III. By considering both the loss and magnetic information in a fifth-order LPTN model, the method in [24] can achieve the estimation accuracy with average error less than 2.5 °C and MAE less than 5 °C, respectively. The calculation speed of the method in [24] is fast with running time of 86.2 μs in DSP (TMS320F28377D). Since the parameters of LPTN model in [24] is identified by PSO algorithm, the parameter dependency of [24] is accordingly lowered. However, the establishment of LPTN model in [24] still requires time-consuming FEA process and special devices to measure the loss information, which increases the algorithm implementation complexity. Aiming at minimizing the parameter dependency, a simplified estimation model is derived in [26] based on three-dimensional (3-D) LPTN and machine temperatures are calculated using the least square method. The estimation accuracy is comparable to [24] with average estimation error less than 2 °C and MSE less than 5.5 °C^2, respectively. With no machine parameters involved, the parameter dependency is eliminated in [26]. The calculation speed of the method in [26] is relatively slow with the calculation time in MATLAB less than 1 s. Due to the need of distributed sensors and mandatory data-collection process, the implementation complexity of [26] is also not negligible.

For the comparisons with the existing data-driven neural-network-based methods [28], [29], the proposed method and data-driven methods [28], [29] share a common advantage of low parameter dependency. Regarding the estimation accuracy, the data-driven method [28] exhibits a relatively low estimation accuracy with MSE less than 6.9 °C^2 and MAE less than 7.92 °C. The estimation accuracy in the data-driven method [29] is further improved with MSE of 0.38 °C^2. In contrast, the proposed integrated model-based and data-driven method achieves superior estimation accuracy with stator and rotor MSEs of 0.07 °C^2 and 0.21 °C^2, respectively. In general, the implementation complexity of data-driven methods is mainly determined by the algorithm complexity, which can be evaluated by many indicators, including the model running time in embedded hardware, training duration, and the amount of training data. In the data-driven method [28], the model running time in Raspberry Pi 3 Model B+ with the main frequency of 1.4 GHz is 8.5 ms. The training duration of [28] on a high-performance GPU (RTX2060 Super) with 957 600 training samples is 21 min. In the data-driven method [29], the model running time in embedded hardware and the training duration are not provided, and 50 000 decision trees need to be trained with 172 000 training samples, which leads to the significant computational burden. By comparison, the model running time of the proposed method in the common industrial microcontroller DSP with the main frequency of 150 MHz is 0.4 ms. Additionally, the training duration of the proposed method on a CPU (i5-1135G7) with 120 000 training samples is 23 min. It is worth mentioning that the proposed method can still achieve a training duration comparable to that of [28] although the performance of the computing device used in the proposed method is significantly lower than [28]. According to the above analysis, the proposed method can be easily deployed in the common industrial microcontrollers with fewer training samples, less training duration, and lower computational burden, which

TABLE III
COMPARISONS OF TEMPERATURE ESTIMATION METHODS

Estimation methods	Estimation accuracy	Calculation speed	Parameter dependency	Implementation complexity
Model-based method I: [24]	Medium-High	Fast	Medium	Medium-Low
Model-based method II: [26]	Medium-High	Medium-Slow	Low	Medium
Data-driven method I: [28]	Medium	Medium-Slow	Low	High
Data-driven method II: [29]	High	Medium-Slow	Low	High
Proposed hybrid-driven method	High	Medium-Fast	Low	Medium

implies the lower implementation complexity of the proposed method. In the aspect of calculation speed, the proposed method exhibits the fastest model running time in comparison with the data-driven methods [28], [29], which can be easily applied in real-time applications.

Based on the above comprehensive comparisons regarding the important performance indexes listed in Table III, it is evident that the proposed method can be conveniently implemented in the common industrial microcontrollers with reliable estimation accuracy, fast calculation speed, and low parameter dependency, which demonstrates the viability and superiority of the proposed method. Compared with the existing model-based and data-driven methods, the proposed integrated method is competitive and perfectly suitable for online temperature estimation of PMSM.

V. CONCLUSION

This article presents an integrated model-based and data-driven method for online precise temperature estimation of PMSM. Unlike the conventional model-based LPTN methods, which requires sophisticated modeling efforts and additional measuring equipment to develop an accurate LPTN model for precise temperature estimation, a simplified LPTN model is established in the proposed method to extract thermal dynamics of PMSM and provide prior temperature knowledge for the ANN compensator. With no requirement for the information regarding the hardly accessible machine structural and material properties, the parameters of the simplified LPTN model in the proposed method can be directly identified in an end-to-end manner based on the easily measured variables, including the relevant temperatures, *d*-*q* axis currents, and rotor speed. Although the accuracy of the simplified LPTN model is sacrificed in the proposed method in exchange for the low parameter dependency, the specifically designed ANN compensator can be utilized to effectively compensate the model uncertainty to guarantee the superior estimation performance of the proposed method. In this way, accurate temperature estimation is fulfilled while maintaining a low computational burden and reduced parameter dependency. Experimental results show that the proposed method achieves excellent estimation performances with stator and rotor MSEs of 0.07 $^{\circ}C^2$ and 0.21 $^{\circ}C^2$, which outperforms the existing state-of-the-art methods. Real-time estimation performed in the common industrial microcontroller DSP shows that the running time of single estimation is 0.4 ms, which is acceptable in practical applications.

REFERENCES

[1] J. Hang et al., "Integration of interturn fault diagnosis and torque ripple minimization control for direct-torque-controlled SPMSM drive system," *IEEE Trans. Power Electron.*, vol. 36, no. 10, pp. 11124–11134, Oct. 2021.

[2] X. Wang, S. Ren, D. Xiao, X. Meng, G. Fang, and Z. Wang, "Fault-tolerant control of open-circuit faults in standard PMSM drives considering torque ripple and copper loss," *IEEE Trans. Transp. Electrific.*, to be published, doi: 10.1109/TTE.2023.3306457.

[3] R. Antonello, M. Carraro, A. Costabeber, F. Tinazzi, and M. Zigliotto, "Energy-efficient autonomous solar water-pumping system for permanent-magnet synchronous motors," *IEEE Trans. Ind. Electron.*, vol. 64, no. 1, pp. 43–51, Jan. 2017.

[4] L. Jin, Y. Mao, X. Wang, L. Lu, and Z. Wang, "Online data-driven fault diagnosis of dual three-phase PMSM drives considering limited labeled samples," *IEEE Trans. Ind. Electron.*, to be published, doi: 10.1109/TIE.2023.3312431.

[5] Z. Zhang, X. Wang, D. Xiao, Y. Zhou, M. He, and Z. Wang, "A novel 3-D space vector modulation strategy for open-end winding PMSM," *IEEE Trans. Ind. Electron.*, to be published, doi: 10.1109/TIE.2023.3314868.

[6] Q. Geng, Z. Li, H. Wang, G. Zhang, and Z. Zhou, "Natural fault-tolerant control with minimum copper loss in full torque operation range for dual three-phase PMSM under open-circuit fault," *IEEE Trans. Power Electron.*, vol. 39, no. 1, pp. 1279–1291, Jan. 2024, doi: 10.1109/TPEL.2023.3323570.

[7] L. Lu, Y. Mao, X. Wang, L. Jin, and Z. Wang, "Maximum-torque optimization control of dual three-phase PMSM in low-frequency and static operations," *IEEE J. Emerg. Sel. Topics Power Electron.*, vol. 11, no. 5, pp. 5268–5278, Oct. 2023.

[8] C. Lai, G. Feng, K. Mukherjee, J. Tjong, and N. C. Kar, "Maximum torque per ampere control for IPMSM using gradient descent algorithm based on measured speed harmonics," *IEEE Trans. Ind. Inform.*, vol. 14, no. 4, pp. 1424–1435, Apr. 2018.

[9] L. Jin, Y. Mao, X. Wang, P. Shi, L. Lu, and Z. Wang, "Optimization-based maximum-torque fault-tolerant control of dual three-phase PMSM drives under open-phase fault," *IEEE Trans. Power Electron.*, vol. 38, no. 3, pp. 3653–3663, Mar. 2023.

[10] S. Nandi, H. A. Toliyat, and X. Li, "Condition monitoring and fault diagnosis of electrical motors—A review," *IEEE Trans. Energy Convers.*, vol. 20, no. 4, pp. 719–729, Dec. 2005.

[11] J. Lopez-Sanz et al., "Nonlinear model predictive control for thermal management in plug-in hybrid electric vehicles," *IEEE Trans. Veh. Technol.*, vol. 66, no. 5, pp. 3632–3644, May 2017.

[12] R. Han et al., "Modulated model predictive control for reliability improvement of extremely low frequency power amplifier via junction temperature swing reduction," *IEEE Trans. Ind. Electron.*, vol. 69, no. 1, pp. 302–313, Jan. 2022.

[13] S. Liu, Q. Wang, G. Zhang, G. Wang, and D. Xu, "Online temperature identification strategy for position sensorless PMSM drives with position error adaptive compensation," *IEEE Trans. Power Electron.*, vol. 37, no. 7, pp. 8502–8512, Jul. 2022.

[14] M. Ganchev, H. Umschaden, and H. Kappeler, "Rotor temperature distribution measuring system," in *Proc. 37th Annu. Conf. IEEE Ind. Electron. Soc.*, 2011, pp. 2006–2011.
[15] S. Stipetic, M. Kovacic, Z. Hanic, and M. Vrazic, "Measurement of excitation winding temperature on synchronous generator in rotation using infrared thermography," *IEEE Trans. Ind. Electron.*, vol. 59, no. 5, pp. 2288–2298, May 2012.
[16] Y. Tang, L. Chen, F. Chai, and T. Chen, "Thermal modeling and analysis of active and end windings of enclosed permanent-magnet synchronous in-wheel motor based on multi-block method," *IEEE Trans. Energy Convers.*, vol. 35, no. 1, pp. 85–94, Mar. 2020.
[17] A. Boglietti, M. Cossale, M. Popescu, and D. A. Staton, "Electrical machines thermal model: Advanced calibration techniques," *IEEE Trans. Ind. Appl.*, vol. 55, no. 3, pp. 2620–2628, May/Jun. 2019.
[18] O. Wallscheid and J. Böcker, "Global identification of a low-order lumped-parameter thermal network for permanent magnet synchronous motors," *IEEE Trans. Energy Convers.*, vol. 31, no. 1, pp. 354–365, Mar. 2016.
[19] C. Kral, A. Haumer, and S. B. Lee, "A practical thermal model for the estimation of permanent magnet and stator winding temperatures," *IEEE Trans. Power Electron.*, vol. 29, no. 1, pp. 455–464, Jan. 2014.
[20] X. Fan, D. Li, R. Qu, and C. Wang, "A dynamic multilayer winding thermal model for electrical machines with concentrated windings," *IEEE Trans. Ind. Electron.*, vol. 66, no. 8, pp. 6189–6199, Aug. 2019.
[21] C. Sciascera, P. Giangrande, L. Papini, C. Gerada, and M. Galea, "Analytical thermal model for fast stator winding temperature prediction," *IEEE Trans. Ind. Electron.*, vol. 64, no. 8, pp. 6116–6126, Aug. 2017.
[22] H. Zhang et al., "Thermal model approach to multisector three-phase electrical machines," *IEEE Trans. Ind. Electron.*, vol. 68, no. 4, pp. 2919–2930, Apr. 2021.
[23] J. Feng, D. Liang, Z. Q. Zhu, S. Guo, Y. Li, and A. Zhao, "Improved low-order thermal model for critical temperature estimation of PMSM," *IEEE Trans. Energy Convers.*, vol. 37, no. 1, pp. 413–423, Mar. 2022.
[24] L. Cao, X. Fan, D. Li, W. Kong, R. Qu, and Z. Liu, "Improved LPTN-based online temperature prediction of permanent magnet machines by global parameter identification," *IEEE Trans. Ind. Electron.*, vol. 70, no. 9, pp. 8830–8841, Sep. 2023.
[25] D. E. G. Erazo, O. Wallscheid, and J. Böcker, "Improved fusion of permanent magnet temperature estimation techniques for synchronous motors using a kalman filter," *IEEE Trans. Ind. Electron.*, vol. 67, no. 3, pp. 1708–1717, Mar. 2020.
[26] Z. Sheng, D. Wang, J. Fu, and J. Hu, "A computationally efficient spatial online temperature prediction method for PM machines," *IEEE Trans. Ind. Electron.*, vol. 69, no. 11, pp. 10904–10914, Nov. 2022.
[27] W. Kirchgässner, O. Wallscheid, and J. Böcker, "Data-driven permanent magnet temperature estimation in synchronous motors with supervised machine learning: A benchmark," *IEEE Trans. Energy Convers.*, vol. 36, no. 3, pp. 2059–2067, Sep. 2021.
[28] W. Kirchgässner, O. Wallscheid, and J. Böcker, "Estimating electric motor temperatures with deep residual machine learning," *IEEE Trans. Power Electron.*, vol. 36, no. 7, pp. 7480–7488, Jul. 2021.
[29] H. Jing et al., "Gradient boosting decision tree for rotor temperature estimation in permanent magnet synchronous motors," *IEEE Trans. Power Electron.*, vol. 38, no. 9, pp. 10617–10622, Sep. 2023.
[30] G. D. Demetriades, H. Z. de la Parra, E. Andersson, and H. Olsson, "A real-time thermal model of a permanent-magnet synchronous motor," *IEEE Trans. Power Electron.*, vol. 25, no. 2, pp. 463–474, Feb. 2010.
[31] H. M. Flieh, R. D. Lorenz, E. Totoki, S. Yamaguchi, and Y. Nakamura, "Dynamic loss minimizing control of a permanent magnet servomotor operating even at the voltage limit when using deadbeat-direct torque and flux control," *IEEE Trans. Ind. Appl.*, vol. 55, no. 3, pp. 2710–2720, May/Jun. 2019.
[32] J. Hang, H. Wu, S. Ding, Y. Huang, and W. Hua, "Improved loss minimization control for IPMSM using equivalent conversion method," *IEEE Trans. Power Electron.*, vol. 36, no. 2, pp. 1931–1940, Feb. 2021.
[33] Z. Ugray et al., "Scatter search and local NLP solvers: A multistart framework for global optimization," *Informs J. Comput.*, vol. 19, no. 3, pp. 328–340, 2007.
[34] D. Ankelhed, A. Helmersson, and A. Hansson, "A quasi-Newton interior point method for low order H-infinity controller synthesis," *IEEE Trans. Autom. Control*, vol. 56, no. 6, pp. 1462–1467, Jun. 2011.
[35] K. Hornik, M. Stinchcombe, and H. White, "Multilayer feedforward networks are universal approximators," *Neural Netw*, vol. 2, no. 5, pp. 359–366, Mar. 1989.
[36] B. M. Wilamowski and H. Yu, "Improved computation for Levenberg–Marquardt training," *IEEE Trans. Neural Netw.*, vol. 21, no. 6, pp. 930–937, Jun. 2010.

Luhan Jin (Student Member, IEEE) received the B.S. degree in communication engineering from Zhengzhou university, Zhengzhou, China, in 2021. He is currently working toward the Ph.D. degree in measuring technology and instrument from the Institute of Optics and Electronics, Chinese Academy of Science, Beijing, China.

His current research interests include the fault diagnosis and tolerant control of motor drives and distributed multiagent system, digital twin modeling and control optimization of motor drives.

Yao Mao (Member, IEEE) received the B.S. degree in automatic control from the Department of Automation, Chongqing University, Chongqing, China, in 2001, and the Ph.D. degree in signal and information processing from the Institute of Optics and Electronics, Chinese Academy of Science, Beijing, China, in 2012.

He has been a Professor with the University of Chinese Academy of Sciences since 2016. His research interests include power electronics, motion control, information fusion, and machine learning.

Dr. Mao was the recipient of Distinguished Scientific Achievement Award by the Chinese Academy of Science in 2011.

Xueqing Wang (Member, IEEE) received the B.S. degree from Tianjin University of Science and Technology, Tianjin, China, in 2014, and the M.S. and Ph.D. degrees from Southeast University, Nanjing, China, in 2016 and 2020, respectively, all in electrical engineering.

From 2018 to 2019, he was a joint Ph.D. with McMaster Automotive Resource Centre, McMaster University, Hamilton, Canada. He is currently an Associate Research Fellow with the College of Electrical Engineering, Sichuan University, Chengdu, China. His research interests include control of multiphase motor and open-winding motor, fault diagnosis and tolerant control of motor drive, and multilevel PWM strategy.

Linlin Lu (Student Member, IEEE) received the B.E. degree in communication engineering from Zhengzhou University, Zhengzhou, China, in 2021. She is currently working toward the M.S. degree in measuring technology and instrument with the Institute of Optics and Electronics, Chinese Academy of Science, Beijing, China.

Her current research interest includes the optimal control of permanent magnet motors.

Zheng Wang (Senior Member, IEEE) received the B.Eng. and M.Eng. degrees from Southeast University, Nanjing, China, in 2000 and 2003, respectively, and the Ph.D. degree from The University of Hong Kong, Hong Kong, in 2008, all in electrical engineering.

From 2008 to 2009, he was a Postdoctoral Fellow with Ryerson University, Toronto, ON, Canada. He is currently a Full Professor with the School of Electrical Engineering, Southeast University, China. He has authored or coauthored more than 80 internationally refereed papers and four books in these areas. His research interests include electric drives, power electronics, and distributed generation.

Dr. Wang received several academic awards including IEEE Power and Energy Society Chapter Outstanding Engineer Award and Best Paper Award of International Conference on Electrical Machines and Systems.